CFD Analysis of Civil Transport Aircraft

Parthsarthi A Kulkarni[1] Dr. Pravin V Honguntikar[2] Vishal S Shirbhate[3]
[1]M. Tech Scholar [2]Professor [3]Scientist C
[1]Department of Thermal Power Engineering [2]Department of Mechanical Engineering
[1,2]Poojya Doddappa Appa College of Engineering Kalburgi, Karnataka, India. [3]National Aerospace Laboratories, Bangalore, Karnataka, India

Abstract— Understanding the motion of air around an object enables the calculations of forces acting on the object. The accurate prediction of aerodynamic coefficient is an important design parameter in preliminary design phase of civil transport aircraft. The common research model utilized by the Drag Prediction Workshop is employed to investigate the accuracy of CFD codes in transonic aerodynamic flow analysis. Solutions are obtained for the wing body configuration. Grid convergence and resolution, mesh topology are considered the primary factors in this study for accurate prediction of aerodynamic coefficients. The current work deals with grid sensitivity studies demonstrated for in-viscid simulations over a typical civil transport aircraft near transonic regime. The commercial grid generation tool ICEM CFD is used for meshing and Euler version of ANSYS FLUENT is used as a solver for numerical computations. The initial study is carried out for CRM model and based on these grid sensitivity studies, typical civil transport aircraft is studied. The lift coefficient value obtained is 0.3389 which is close to value of 0.4 reported in experiment. The experimental data taken from drag prediction workshop for the common research model are well agreed with CFD results.

Key words: CRM, CFD, ICEM CFD, Ansys Fluent

I. INTRODUCTION

Effective use of computational fluid dynamics (CFD) is a key ingredient in successful design of modern commercial and military aircraft. The combined pressures of market competitiveness, dedication to the highest of safety standards, and desires to remain a profitable business enterprise all contribute to make intelligent, extensive, and careful use of CFD a major strategy for product development. The application of CFD today has revolutionized the process of aerodynamic design [1]. CFD has joined the wind tunnel and flight test as primary tools of the trade.[1-4] Because of the tremendous cost involved (and potential risk) in flight testing, modern aircraft development places heavy focus on the use of CFD and the wind tunnel prior to flight. Particularly, CFD is used to provide understanding and insight as to the source of undesirable flight characteristics, whether they are observed in sub-scale model testing or in the full-scale flight testing. Collectively, flight testing, wind tunnel testing, and CFD all contribute to minimizing risk and uncertainty in a new airplane product. Therefore, validation and improvement of CFD technology is a requirement and an ever-present necessity for aerospace companies. The main focus of DPW4 [5] was cruise drag prediction for the NASA Common Research Model (CRM). The CRM is representative of a commercial wing-body transport configuration and is shown in Figure 1. It was jointly designed by NASA and Boeing, the overall design, fabrication, and testing was led by NASA and the detailed aerodynamic design was led by the Boeing Company.

During the first decade of the 21st Century, the AIAA CFD Drag Prediction Workshop Series (DPW) [6-10] has become an invaluable resource for Computational Fluid Dynamics (CFD) and Aerodynamic Design (AD) communities worldwide. One of the charter objectives of DPW is to assess the state-of-the-art of CFD accuracy across the industry. One approach utilized in attempts to accomplish this objective has been to conduct grid-convergence studies. Although other factors as the quality of the mesh is of paramount importance play a role in the accuracy of CFD simulation. DPW-V will include a grid-convergence test-case which is based on a unified grid system about the wing-body configuration of the NASA Common Research Model (CRM).

II. CRM MODEL GEOMETRY SPECIFICATIONS

The baseline wing-body (WB) configuration for DPW-V is that of the NASA Common Research Model (CRM). The CRM is representative of a contemporary transonic commercial transport designed to cruise at M = 0.85 and CL = 0.5 at a nominal altitude of 37,000 ft.

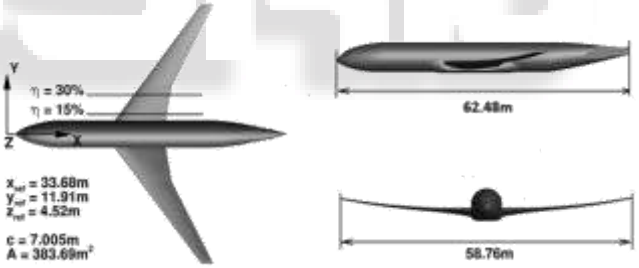

Fig. 1: Three Views of CRM Model

The aspect ratio is 9.0, the leading edge sweep angle is 35 deg, the wing reference area (S) is 3.01 ft2 (0.2796 m2), the wing span (b) is 62.46 inches (1.586m), and the mean aerodynamic chord (c) is 7.45 inches (0.1892m). The model moment reference centre is located 35.8 inches (0.9093m) back from the fuselage nose and 1.177 inches (0.0298m) below the fuselage centerline.

III. COMPUTATIONAL FLUID DYNAMICS (CFD)

Computational fluid dynamics, usually abbreviated as CFD, is a branch of fluid mechanics that uses numerical methods and algorithms to solve and analyze problems that involve fluid flows. Computers are used to perform the calculations required to simulate the interaction of liquids and gases with surfaces defined by boundary conditions using ANSYS FLUENT 14. The technique is very powerful and spans a wide range of industrial and non-industrial areas.

A. Governing Equations:

The governing equations of fluid flow represent mathematical statements of the conservation laws of physics:

1) The mass of a fluid is conserved
2) The rate of change of momentum equals the sum of the forces on a fluid particle (Newton's second law)
3) The rate of change of energy is equal to the sum of the rate of heat addition to and the rate of work done on a fluid particle (first law of thermodynamics).

B. The Mass Conservation Equation:

The equation for conservation of mass, or continuity equation, can be written as follows:

$$\frac{\partial \rho}{\partial t} + \nabla \cdot (\rho \vec{v}) = S_m \quad (1)$$

The above equation is the general form of the mass conservation equation and is valid for incompressible as well as compressible flows. The source 'Sm' is the mass added to the continuous phase from the dispersed second phase (e.g., due to vaporization of liquid droplets) and any user-defined sources.

C. Momentum Conservation Equation:

Conservation of momentum is described by

$$\frac{\partial}{\partial t}(\rho \vec{v}) + \nabla \cdot (\rho \vec{v} \vec{v}) = -\nabla p + \rho \vec{g} + \vec{F} \quad (2)$$

Where p is the static pressure and ρg and are the gravitational body force and external body forces (e.g., forces that arise from interaction with the dispersed phase), respectively.

D. Energy Conservation Equation:

Conservation of energy is described by

$$\frac{\partial}{\partial t}(\rho E) + \nabla \cdot (\vec{v}(\rho E + p)) = -\nabla \cdot \left(\sum_j h_j J_j \right) + S_h \quad (3)$$

IV. METHODOLOGY

CFD analysis and study of results are carried out in 3 steps: Pre-processing, solving and post-processing.

Geometry of the CAD model is created in CATIA V5 R20 modeling software followed by unstructured mesh using mesh tool. The details of the mesh are:

A. Grid Generation for CRM

Accurate representations of the geometry, along with generating a high quality mesh, are critical steps in obtaining an acceptable solution. The grid [12] sensitivity study was carried out by generating three different meshes (coarse, medium and fine). The mesh details associated with each solver is shown in Table 1. Finally, the mesh which gives results close to experimental will be chosen for detail CFD analysis.

Grid type	Coarse	Medium	Fine
Elements	2948265	7457647	16737687
Nodes	516726	1298910	2951863
Surface mesh	All Tri	All Tri	All Tri
Volume mesh	All Tetrahedrons	All Tetrahedrons	All Tetrahedrons
Mesh type	Patch dependent	Patch dependent	Patch dependent

Table 1: Description of the meshes for ANSYS FLUENT

The IGES file was imported in ICEM-CFD [13] with tri tolerance of 0.0001 and topo tolerance of 0.001. Geometry clean up carried out in ICEM with build topology tolerance 0.2

GRID	GLOBAL ELEMENT SIZE
Fine grids	1024
Medium grids	2048
Coarse grids	4096

Table 2: Global Element Size for Different Grids

The global element sizes of three grids are mentioned in table 2. The different surface mesh over the CRM model is shown in figure 2, 3, 4 respectively.

Fig. 2: Coarse Mesh On CRM

Fig. 3: Medium Mesh on CRM

Fig. 4: Fine Mesh on CRM

The surface mesh was generated with triangular elements using patch dependent method. The volume mesh was selected with tetra/mixed mesh as a volume meshing parameter and tetrahedral elements are generated using octree method.

B. Grid Generation for RTA Model:

ICEM-CFD grid generator was used to develop the mesh for ANSYS FLUENT. The grid sensitivity study was carried out by generating three different meshes (coarse, medium and fine). The mesh details associated with each solver is shown in Table 3

Grid type	Coarse	Medium	Fine
Elements	6034373	7354408	10205649
Nodes	1050813	1285015	1784463
Surface mesh	All Tri	All Tri	All Tri
Volume mesh	All Tetrahedrons	All Tetrahedrons	All Tetrahedrons
Mesh type	Patch dependent	Patch dependent	Patch dependent

Table 3: Description of the meshes for ANSYS FLUENT

GRID	GLOBAL ELEMENT SIZE
Fine grids	8192
Medium grids	16384
Coarse grids	32768

Table 4: Global element size for different grids

The global element sizes of three grids are mentioned in table 4. The different surface meshes over the RTA model are shown in figure 5, 6, 7 respectively.

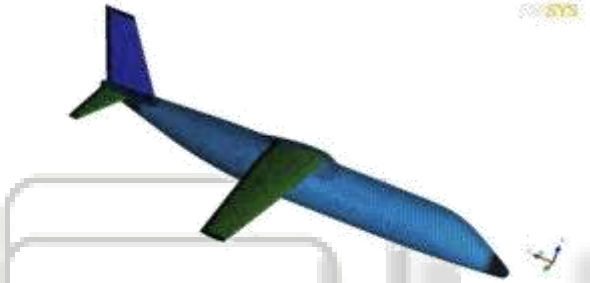

Fig. 5: Coarse Mesh on RTA Model

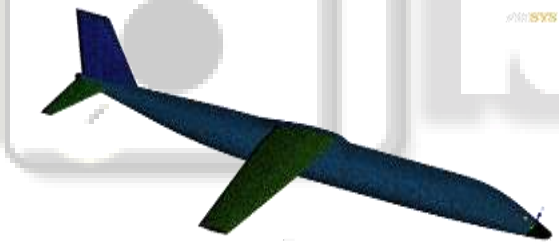

Fig. 6: Medium Mesh on RTA Model

Fig. 7: Fine Mesh on RTA Model

C. Flow Conditions:

The Flow conditions specified in this project are as given under

D. Flow Conditions for CRM:

- Grid Convergence study at Mach = 0.85
- AOA = 2^0
- Chord Reynolds Number RE = $5x10^6$ based on C_{REF} = 7.005 m
- Reference Temperature = 310.928 K
- Moment reference center is X_{REF} = 33.6779 m, Z_{REF} = 4.51993m.
- Reference pressure = 201326.9 Pa.

E. Flow Conditions for RTA Model

- Grid Convergence study at Mach = 0.5
- AOA =0^0, 2^0, 5^0,10^0.
- Reference Temperature = 238.62 K
- Moment reference center is X_{REF} = 11.7934 m.
- Reference pressure = 37599 Pa

F. Solver Settings for CRM:

The solver used for the study is ANSYS FLUENT with finite volume approach. Mesh generated in ICEM-CFD is imported in Ansys fluent. The mesh was scaled from inches to metres. The scaling was required as the basic CAD model was available in inches. The geometry parameters and flow conditions are given in SI units in the literature. Hence, the conversion of mesh is carried out from inches to metre.

G. Boundary Condition:

The boundary condition is the initializing condition used to start the solver in that

1) Body of aircraft is set to WALL.
2) Far-field is set to pressure far-field
3) Symmetry is set to symmetry

H. Solver Settings for RTA Model:

The solver settings used for RTA model are same as that of CRM model followed by appropriate boundary conditions

V. Results and Discussion

A. Contour Results for CRM Model:

The solution iteration was set to auto save after every 500 iterations and solution calculation was set to a total 2500 iterations.The iterations were stopped when the CL, CD, Cm monitor residual values showed alternate fluctuation of same bandwidth.

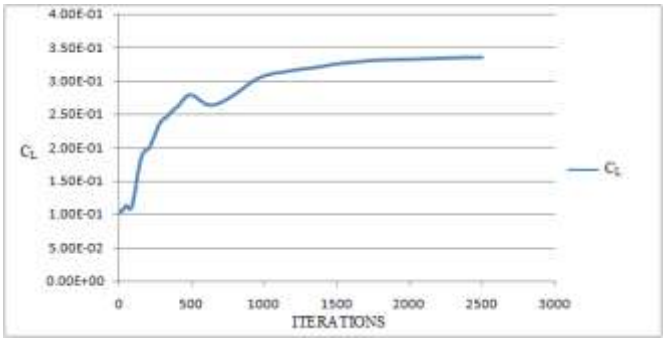

Fig. 8: Lift Convergence History

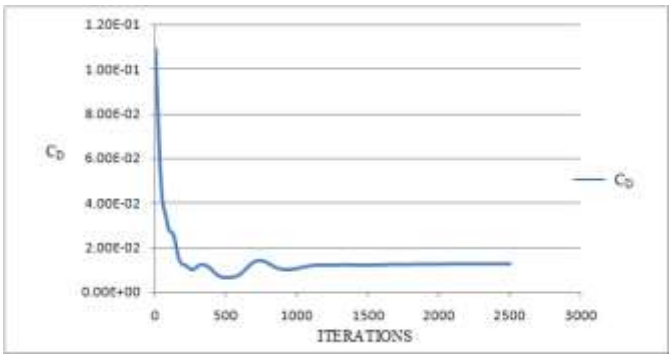

Fig. 9: Drag Convergence History

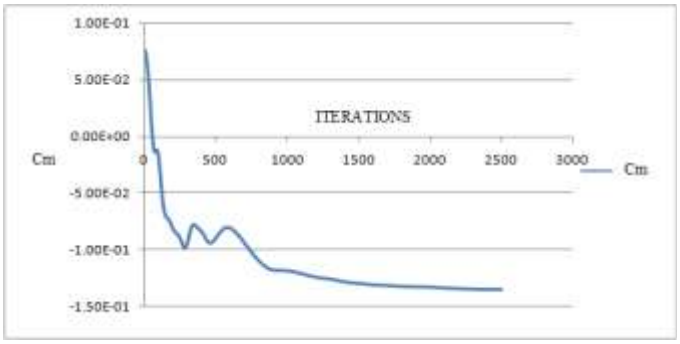

Fig. 10 : Moment Convergence History

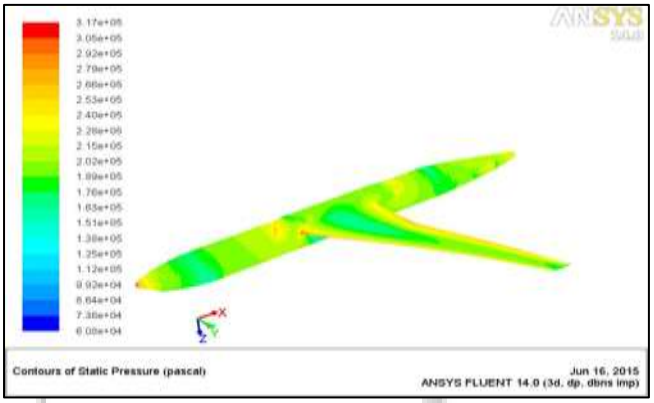

Fig. 11: Pressure Contour of the CRM with Static Pressure

The Figure 11 shows pressure contour of the CRM with static pressure, here the pressure value ranges from 6.08e+4 (min) to 3.17e+5 (max), while the intermediate pressure ranges 1.89e+5 to 2.02e+5.The magnitude of the static pressure is found to be high on the nose, leading & trailing edges of the aircraft.

Fig. 12: Velocity Vector Colored by Velocity Magnitude.

The Figure 12 shows velocity vector of the CRM with velocity magnitude, here the velocity value ranges from 5.07e+0 (min) to 6.14e+2 (max), while the intermediate velocity ranges 3.09e+2 to 3.70e+2. The magnitude of the velocity is found to be high on the upper side of the aircraft wing.

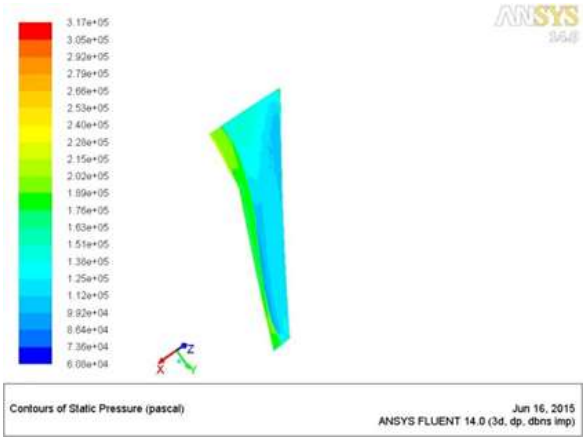

Fig. 13: Pressure Distribution on Upper Side of Wing

The Figure 13 shows pressure distribution on lower side of wing , here the pressure value ranges from 6.08e+4 (min) to 3.17e+5 (max), while the intermediate pressure ranges 1.89e+5to 2.02e+5.

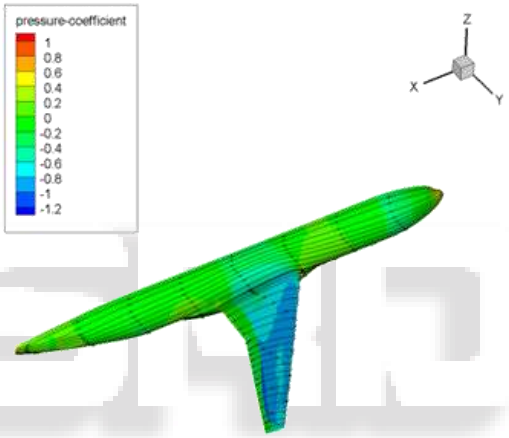

Fig. 14: Pressure Coefficient Distribution and Surface Streamlines Over the CRM

The figure 14 shows the pressure coefficient distribution on the surface of the CRM, here the pressure coefficient value ranges from -1.2 (min) to 1 (max).The pressure coefficient is found to be high on the nose and wing body junction, while the minimum value exists on the upper surface of the wing.

The following data are calculated using Ansys fluent solver using inviscid model. The results obtained in the solver showed close match to experimental results.
The outcome of the study is mentioned below:

- Lift coefficient, C_L: 0.3389
- Drag coefficient, C_D: 0.0129

AOA 2^0	Experimental value	Fine mesh	Medium mesh	Coarse mesh
C_L	0.4	0.3389	0.3388	0.336
C_D	0.025	0.0129	0.0131	0.0137

Table 5: Comparsion between CFD and Experimental Results

B. Contour Results for RTA model:

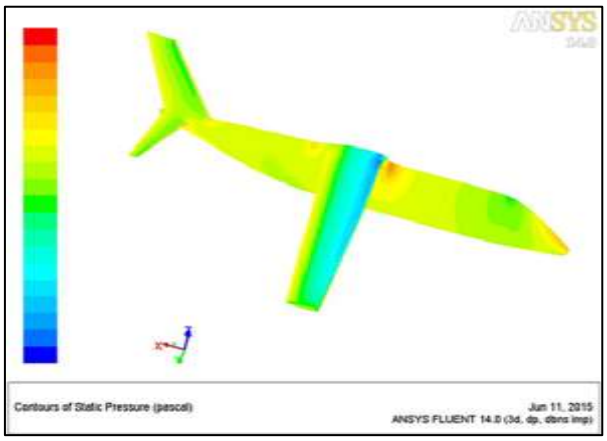

Fig. 15: Surface Pressure Contours over RTA Model at Mach number 0.5

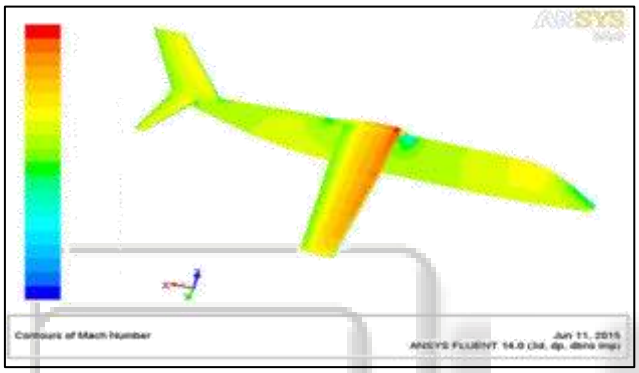

Fig. 16: Surface Velocity vectors over RTA model at mach number 0.5

Fig. 17: Surface Pressure Distribution on Lower Side of Wing

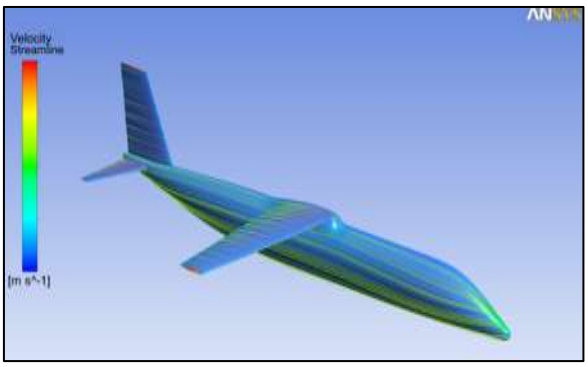

Fig. 18: Velocity streamlines over RTA Model

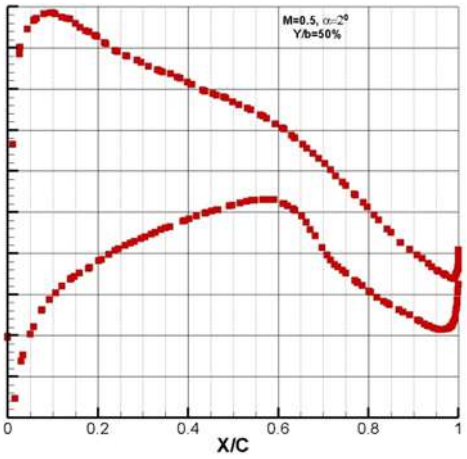

Fig. 19: Pressure coefficient distribution over wing surface at Y/b = 50%.

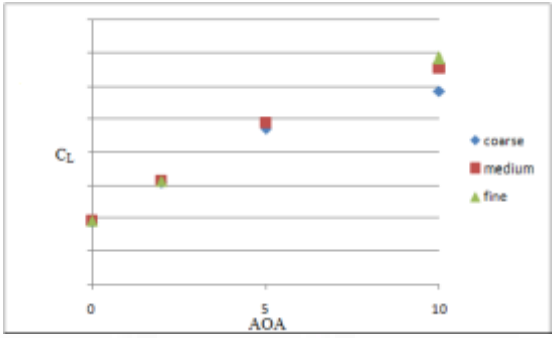

Fig. 20: Variation of CL with AOA

The figure 20 shows the variation of lift coefficient CL with angle of attack.The lift coefficient is found to increase with increase in angle of attack.

C. Comparison of lift co-efficient value with the experimental results:

An experimental investigation data [14] is collected for the common research model, which showed the lift co-efficient (CL) value of 0.4, and the results for simulation obtained is CL=0.3389 and are well comparable. A comparison is made with the experimental results to the common research model. The initial study is carried out for CRM model and based on these grid sensitivity studies, typical civil transport aircraft is studied. The aerodynamic coefficients are obtained for the RTA model same as that of CRM model. The CRM model provides a baseline for the aerodynamic analysis as experimental results were readily available.

VI. CONCLUSION

The aerodynamic coefficients are calculated using ANSYS FLUENT solver using in-viscid model. The result obtained in the solver showed aerodynamic coefficients value close to experimental result.

Based on the CFD study carried out on CRM model & RTA model following conclusions are drawn

1) Fine mesh is considered to be most suitable mesh for CFD analysis.
2) The medium mesh can be used for further CFD analysis. The medium mesh can also be used for generating boundary layers over body surafce for generating mesh to be used further for computing viscous flows.

3) The medium mesh can also be used for generating boundary layers near wall for computing viscous flows.

REFERENCES

[1] Rubbert, P. E., "AIAA Wright Brothers Lecture: CFD and the Changing World of Airplane Design" ICAS 94-0.2, September 1994.
[2] Tinoco, E. N., "The Changing Role of Computational Fluid Dynamics in Aircraft Development," AIAA Paper 98-2512, June 1998.
[3] [Johnson, F. T.,Tinoco, E. N., and Yu, N. J., "Thirty Y**e**ars of Development and Application of CFD at Boeing Commercial Airplanes, Seattle," AIAA Paper 2003-3439, June 2003.
[4] Goldhammer, M. I., "Boeing 787 Design for Optimal Airplane Performance," CEAS/KATnet Conference on Key Aero-dynamic Technologies, Bremen, Germany, June 2005.
[5] Vassberg, J. C., Dehaan, M. A., Rivers, S. M., and Whals, R. A."Development of a Common Research Model for Applied CFD Validation Studies," AIAA Paper 2008-6919, August 2008.
[6] 1st AIAA CFD Drag Prediction Workshop, San Francisco. Accessed2000"http://aaac.larc.nasa.gov/tsab/cfdlarc/aiaadpw/Workshop3/workshop3.html"
[7] 2nd AIAA CFD Drag Prediction Workshop, San Francisco. Accessed2003"http://aaac.larc.nasa.gov/tsab/cfdlarc/aiaadpw/Workshop3/workshop3.html"
[8] 3rd AIAA CFD Drag Prediction Workshop, San Francisco accessed11November2012"http://aaac.larc.nasa.gov/tsab/cfdlarc/aiaadpw/Workshop3/workshop3.html"
[9] 4th AIAA CFD Drag Prediction Workshop, San Antonio, TX,June2009"http://aaac.larc.nasa.gov/tsab/cfdlarc/aiaadpw/Workshop4/workshop4.html"aiaadpw@gmail.com, accessed 11 November 2012.
[10] 5th AIAA CFD Drag Prediction Workshop, San Antonio, TX,June2009.http://aaac.larc.nasa.gov/tsab/cfdlarc/aiaadpw/Workshop4/workshop4.html,aiaadpw@gmail.com, accessed 11 November 2012.
[11] C.P. van Dam., "Different methods of drag prediction," AIAA Paper 2007-0255, 45th AIAA Aerospace Sciences Meeting and Exhibit, Reno, NV, January 2004.
[12] Vishal S. Shirbhate, "Reynolds Averaged Navier-Stokes Analysis for Civil Transport Air aircraft using Structured and Unstructured grids", Proceedings, 14th Annual CFD Sympo- possium , Indian Institute of Science, Bangalore, CP-054,10th – 11th August 2012
[13] "ICEM-CFD help engine" by ANSYS
[14] Brodersen, O., Eisfeld, B., Raddatz, J., and Frohnapfel, P., "DLR Results from the Third AIAA CFD Drag Prediction Workshop," AIAA Paper 2007-0259, 45th AIAA Aerospace Sciences Meeting and Exhibit, Reno, NV, January 2007

